Molecular and cellular responses to renal injury : a (phospho)-proteomic approach

Graauw, M. de

Phospho-proteomics of renal cell injury

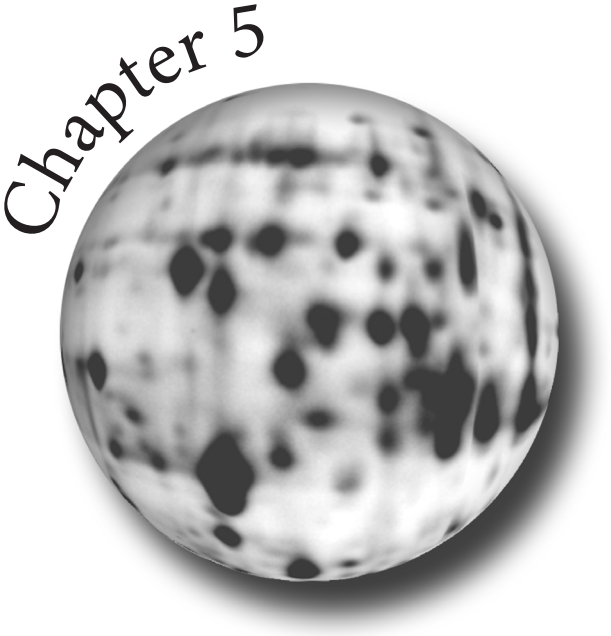

Nephrotoxicant-induced actin reorganization, lamellipodia formation and apoptosis depends on tyrosine kinase activity and involves phosphorylation of actin-related protein 2

Marjo de Graauw[1], Sylvia Le Dévédec[1], Ine Tijdens[1], Mirjam Smeets[2], André M. Deelder[2], Bob van de Water[1]

[1]*Division of Toxicology, Leiden/Amsterdam Center for Drug Research, Leiden University, P.O. Box 9502, 2300 RA, Leiden, The Netherlands and* [2] *Biomolecular Mass Spectrometry Unit, Department of Parasitology, Leiden University Medical Center, P.O. Box 9600, 2300 RC Leiden, The Netherlands.*

ABSTRACT

Using phospho-tyrosine proteomics we identified proteins that were differentially phosphorylated prior to renal cell detachment and apoptosis. Treatment of primary cultured rat proximal tubular epithelial cells with the model nephrotoxicant 1,2-dichlorovinyl-cysteine (DCVC) resulted in F-actin reorganization, followed by cell detachment and apoptosis. The DCVC-induced cell injury was prevented by a general inhibitor of protein tyrosine kinases, genistein, and enhanced by an inhibitor of protein tyrosine phosphatases, vanadate. In addition, DCVC caused lamellipodia formation prior to apoptosis, which was blocked by inhibition of tyrosine kinases. Phospho-tyrosine proteomics revealed that DCVC-induced renal cell apoptosis was preceded by changes in the tyrosine phosphorylation status of a subset of proteins, as identified by MALDI-TOF-MS/MS. The major differentially tyrosine phosphorylated protein was actin-related protein (Arp) 2, while phosphorylation of Arp3 was not affected. Arp2 was located in the lamellipodia that were formed prior to the onset of apoptosis. Since DCVC-induced cell detachment and apoptosis is regulated by tyrosine kinases, we propose that alterations in tyrosine phosphorylation of a subset of proteins, including Arp2 play a role in the regulation of the F-actin reorganization and lamellipodia formation that precede renal cell apoptosis caused by nephrotoxicants.

INTRODUCTION

Renal proximal tubular epithelial (RPTE) cells are an important target for a variety of chemicals, nephrotoxic medicines as well as ischemia/reperfusion injury [1-3]. (Sub)-lethal injury of RPTE cells is associated with loss of cell-extracellular matrix (ECM) and cell-cell interactions [4,5]. Normally, these interactions are maintained by the F-actin cytoskeletal network, but during renal cell injury, the organization of the F-actin cytoskeleton is lost [6,7], resulting in redistribution of integrins, disturbance of focal adhesions and disruption of intercellular adhesions [8-11]. The maintenance of cell adhesions is important for cell survival, whereas loss of RPTE cell adhesion results in the onset of apoptosis [4,5]. *In vivo*, renal injury is associated with loss of cell adhesion and apoptosis, which both seem important in the pathogenesis of acute renal failure [3,12]. Little is known about the molecular mechanisms by which renal cell injury causes cell detachment and the consequences for cell survival.

Protein tyrosine kinases and phosphatases regulate the phosphorylation of proteins located at both cell-cell and cell-ECM contact sites [13-15]. Cell stressors such as nephrotoxicants or ATP depletion perturb protein tyrosine phosphorylation (pTyr), thereby altering the functional state of these cell contact sites [13,14,16]. This suggests that changes in protein pTyr may determine the outcome of renal cell injury [17]. Indeed, pharmacological inhibition of tyrosine kinases prevent nephrotoxicity and renal cell death. For example, the tyrosine kinase inhibitor AG1714 inhibited cisplatin-induced nephrotoxicity [18]. Chemical anoxia in LLC-PK1 cells resulted in increased pTyr, which was blocked by the tyrosine kinase inhibitors genistein, herbimycin A and tyrphostin, thereby providing protection against chemical-anoxia-induced cell death [19].

Adhesion of cells to the ECM or neighboring cells is mediated through focal adhesions (FA) or adherens junctions (AJ). FA formation is regulated by integrin clustering at sites of contact, which in turn results in pTyr and activation of F-actin associated proteins like focal adhesion kinase (FAK), Src kinase and paxillin [20]. Previous studies [8,9] showed that the levels of phosphorylated FAK and paxillin decreased during nephrotoxicant-induced renal cell injury. This is associated with loss of FAs and actin stress fibers and precedes the onset of apoptosis. In addition, expression of a deletion mutant of FAK (GFP-FAT) resulted in enhanced toxicant-induced renal cell injury and apoptosis [8].

The AJs consist of E-cadherin proteins that link two cells in a zipper-like way. E-cadherin is connected to the F-actin cytoskeletal network through catenins [21]. The function of both existing and assembling cell-cell adhesions is regulated by tyrosine phosphorylation. ATP depletion of proximal tubular cells resulted in loss of cell-cell interaction, which was associated with hyper-phosphorylation of β-catenin and plakoglobin [16,17]. This phosphorylation was enhanced by vanadate, a tyrosine phosphatase inhibitor and inhibited by genistein, a general tyrosine kinase inhibitor [17].

Although the role of some tyrosine phosphorylated proteins in renal cell injury has been established, many of these proteins remain unknown. To identify differentially phosphorylated proteins during nephrotoxicant-induced renal cell injury more generally, we used phospho-tyrosine proteomics. This technique is based on high resolution

two-dimensional (2D) SDS-PAGE in conjunction with 2D immunoblot analysis with anti-pTyr antibody [22,23]. To investigate the effects of altered pTyr in renal cell injury and apoptosis, we exposed primary cultured RPTE to the model nephrotoxicant S-(1,2-dichlorovinyl)-L-cysteine (DCVC) [7,25-27]. DCVC is metabolized by a β-lyase to a reactive acylating metabolite that covalently modifies cellular macromolecules [28]. This bio-activation is important for DCVC-induced cytotoxicity. Apoptosis of RPTE caused by DCVC treatment is preceded by disorganization of the F-actin cytoskeletal network and tyrosine dephosphorylation of the FAK and paxillin [7,9]. Thus, DCVC is a useful agent to study the effects of altered pTyr on cell detachment and apoptosis of primary cultured RPTE.

Our data show that DCVC-induced cell injury is associated with an imbalance in tyrosine kinase and phosphatase activity, resulting in alterations in protein pTyr of a subset of proteins, including actin-related protein 2 (Arp2). This altered phosphorylation may be important for renal cell toxicity, but also for other types of organ toxicities, which are directly related to the formation of reactive metabolites.

MATERIALS AND METHODS

Materials

Dulbecco's modified Eagles medium/Ham's F12, PBS, cholera toxin, insulin and penicillin/streptomycin/amphotericin B (PSA) were from Invitrogen. Fetal bovine serum was from Life Technologies (Grand Island, NY). Collagen (type I, rat tail) and epidermal growth factor (EGF) were from Upstate Biotechnology (Lake Placid, NY). Genistein was from Sigma (St. Louis, MO). N,N'-Diphenyl-p-phenylenediamine (DPPD) was from Kodak (Rochester, NY). DCVC was synthesized as described previously [29].

Isolation and culture of RPTE and LLC-PK1 cells

RPTE cells were isolated from male Wistar rats (200-250 g) by collagenase H (Sigma) perfusion and separated by density centrifugation using Nycodenz (Sigma) as described previously [27,30]. Cells were cultured on collagen coated dishes in Dulbecco's modified Eagles medium/Ham's F12 containing 1% (v/v) fetal bovine serum, 0.5 mg/ml bovine serum albumin, 10 μg/ml insulin, 10 ng/ml epidermal growth factor, 10 ng/ml cholera toxin and 1% (v/v) penicillin, streptomycin and amphotericin B (PSA). RPTE were maintained at 37 °C in a humidified atmosphere of 95% air/5% CO2 and fed every other day. Cells were used for experiments after they had reached confluence 6-9 days after plating. The porcine renal epithelial cell line LLC-PK1 cells were maintained in DMEM supplemented with 10% (v/v) FCS and penicillin/streptomycin at 37°C in a humified atmosphere of 95% air and 5% carbon dioxide. For preparation of stable GFP-actin expressing cell lines, LLC-PK1 cells were transfected with 0.8 μg DNA of pEGFP-actin (Clontech) using Lipofectamine-Plus reagent according to the manufacturer's procedures (Life Technologies, Inc). Stable transfectants were selected using 800 μg/ml G418. Individual clones were picked and maintained in complete medium containing 100 μg/ml G418. Clones were analyzed for expression of GFP-actin using immunofluorescence.

Cell treatment conditions

Confluent monolayers of RPTE in collagen (MatTek Corp.) coated glass coverslips containing 24-well dishes, 6 wells or 10 cm dishes were washed with PBS once. Thereafter, cells were treated with DCVC in phenol red free Hanks' balanced salt solution (137 mM NaCl, 5 mM KCl, 0.8 mM MgSO4·7H2O, 0.4 mM Na2HPO4·2H2O, 0.4 mM KH2PO4, 1.3 mM CaCl2, 4 mM NaHCO3, 25 mM HEPES, 5 mM D-glucose, pH 7.4) for indicated time periods in the presence of the antioxidant DPPD (10 μM), which blocks the necrotic pathway, but allows the onset of apoptosis.

Cell cycle analysis

Apoptosis was determined by cell cycle analysis. Briefly, both floating and trypsinized adherent cells were pooled and subsequently fixed in 90% ethanol (-20 °C). After washing cells twice with PBS-EDTA (1mM), cells were resuspended in PBS/EDTA containing 7.5 μM propidium iodide and 10 μg/ml RNase A. After 30 min incubation at room temperature the cell cycle was analyzed by flow cytometry (FACS-Calibur, Becton Dickinson), and the percentage of cells present in sub-G0/G1 was calculated using Cellquest software (Becton Dickinson).

Western blotting

Cells were harvested as described previously 8. Primary antibody incubation was performed overnight at 4 °C using monoclonal PY99 (0.04 μg/ml, Santa Cruz) antibody. Thereafter blots were incubated with horseradish peroxidase conjugated secondary antibody (GE Healthcare) in TBS-T for 1h at room temperature. Protein signals were detected with ECL-plus method (GE Healthcare) followed by scanning of the blots with a Typhoon 9400 (GE Healthcare).

Immuno-fluorescence and imaging techniques

For immuno-fluorescence studies cells were cultured on collagen coated glass coverslips in 24-well dishes. After DCVC treatment cells were fixed with 3.7% formaldehyde for 10 min followed by 3 washes with PBS. After cell permeabilization and blocking with TBP (PBS, 0.2% (w/v) Triton X-100, 0.5% (w/v) bovine serum albumin, pH 7.4), cells were stained for β-catenin (0.25 μg/ml, Transduction Lab) or PY99 (0.2 μg/ml, Santa Cruz) overnight at 4 °C. Cells were washed three times with TPB and subsequently incubated with Alexa-488-labeled goat anti-mouse (1 μg/ml) in combination with rhodamine-phalloidin (0.3 unit/ml, Molecular Probes) to label the F-actin cytoskeletal network, and Hoechst 33258. Cells were mounted on glass slides using Aqua-Poly/Mount (Polysciences Inc.). Cells were analysed using a Bio-Rad Radiance 2100 confocal laser scanning system equipped with a Nikon Eclipse TE2000-U inverted microscope and a 60X Plan Apo (NA 1.4; Nikon) oil-emersion objective. Images were processed with Paint Shop Pro 7.

For live cell imaging, EGFP-actin expressing LLC-PK1 cells were plated on tissue culture dishes containing a collagen-coated coverslip for 24 h in serum free DMEM medium. Cells were exposed to DCVC (1mM) in the presence of DPPD (10 μM) at 37 °C

in 5 % CO_2 for 5 hours in a climate control unit built up on the stage of a Nikon Eclipse TE2000-U inverted microscope. Images were typically taken at 5 min interval using a Bio-Rad Radiance 2100 confocal system with a 60 X Plan Apo (NA 1.4; Nikon) objective lens. Image acquisition was controlled using the Laser Sharp software (Bio-Rad) in combination with an in house developed macro to maintain auto-focus. Movies were processed with Image-Pro (R) Plus (Version 5.1; Media Cybernetics).

Preparation of cell extracts for 2D

Cells were lysed in urea lysis buffer (8M urea, 2M thiourea, 4% (w/v) CHAPS, 10 mM Tris pH 8.0 and 65 mM DTT) and placed on ice for 30 min. The extracts were syringed several times followed by a 15 min centrifugation (10,000 rpm, 10 °C). The protein concentration was determined using a Bradford assay with IgG as a standard. For each sample 150 µg of protein was resuspended in urea lysis buffer containing 0.5 % (v/v) IPG-buffer (Amersham). All samples were prepared and run in quadruplicate according to Görg [31].

Protein separation by 2D gel electrophoresis and 2D image analysis

For isoelectric focusing, 24 cm immobilized pH gradient (IPG) strips pH 3-10 NL (GE Healthcare) were rehydrated with the urea samples at 30V for 12 hours. Isoelectric focusing was performed at room temperature using the Ettan IPGphor IEF system (GE Healthcare). A gradient of 500 to 8000 V was applied over 2 h followed by a constant voltage of 8000 V for 60 kVh. After focusing, the IPG strips were equilibrated at RT for 10 min in equilibration buffer (6 M urea, 2% (w/v) SDS, 1% (w/v) DTT, 30 % (v/v) glycerol and 50 mM Tris pH 6.8). The equilibrated IPG strips were transferred onto 20x26 cm 9% uniform PAGE gels for separation of proteins based on molecular weight. Gels were run in a Hoeffer DALT 10 gel system (GE Healthcare) overnight at 10 °C at a constant amperage of 25 mA per gel. Gels were removed from the plates and either fixed in 30% MeOH / 7.5% acetic acid for subsequent Sypro ruby staining (Molecular Probes) or transferred to nitrocellulose membrane (Schleicher and Schuell) overnight at 4 °C. Western blotting was performed as described under 'Western blotting'.

All generated images were exported as .tif files for further analysis of protein and phosphorylation profiles. Differences in tyrosine phosphorylation were detected visually by overlaying the images using Adobe Photoshop and quantitatively by PDQuestTM 2D Gel Analysis Software (Bio-Rad Laboratory, Inc.). All phospho-tyrosine (PY) profiles were aligned with total protein profiles (Sypro ruby images) to be able to mark proteins undergoing changes in tyrosine phosphorylation. Matched spots from triplicate blots that could be detected on the associated Sypro ruby stained gel were excised from the gel and identified by MALDI-MS(-MS) (Ultraflex time-of-flight, Bruker Daltonics) with peptide mass fingerprinting.

In-gel digestion

Spots picked from Sypro ruby stained gels were cut in small pieces, washed in 10 µl 50 % acetonitril for 15 min followed by an additional wash in 100 % acetonitril. Spots were dried in a speedvac and incubated for 30 min on ice in 5 µl 5 ng/µl trypsin (Promega)

50 mM NH4HCO3. After addition of 50 mM NH4HCO3 so that gel pieces were covered with liquid, tryptic digestion was performed overnight at 37 °C. TFA was added to a final concentration of 0.1% (v/v). A 1 µl aliquot was spotted onto a MALDI target plate using a C18 Zip-Tip (Millipore) for desalting and dihydroxybenzoic acid as a matrix. Analysis of the tryptic peptides was carried out using a MALDI-MS(-MS) (Ultraflex, Bruker Daltonics). Data was analyzed with Flexanalysis 2.0 and Biotools 2.2 (Bruker Daltonics) followed by Mascot search.

Statistical analysis

Student's t-test was used to determine if there was a significant difference between two means ($p<0.05$). When multiple means were compared, significance was determined by one-way analysis of variance (ANOVA; $p<0.05$). For ANOVA analysis, letter designations are used to indicate significant differences. Means with a common letter designation are not different; those with a different letter designation are significantly different from all other means with different letter designations.

RESULTS

DCVC-induced cell detachment and apoptosis is dependent on increased protein tyrosine kinase activity

To determine whether differential regulation of protein tyrosine phosphorylation is important in renal cell injury, primary cultured RPTE were exposed to the model nephrotoxicant DCVC in combination with genistein, a general tyrosine kinase inhibitor and/or vanadate, a general tyrosine phosphatase inhibitor. Treatment of RPTE with DCVC for 4 h resulted in cell rounding, indicating cell detachment of these cells from their substratum and disruption of intercellular adhesion (**Fig. 1A**). No cell detachment was observed in control RPTE. Loss of cell adhesion is often associated with the onset of apoptosis. Indeed, DCVC-induced cell detachment was associated with 36 % apoptosis after 8 h of exposure, compared to 9 % apoptosis of control RPTE (**Fig. 1B**).

Inhibition of protein tyrosine kinase activity by genistein almost completely prevented cell detachment and apoptosis of RPTE, indicating that DCVC-induced renal cell injury might be linked to tyrosine kinase activation (**Fig. 1A-B**). In turn, inhibition of protein tyrosine phosphatase activity by vanadate resulted in enhanced cell rounding and a slight increase in apoptosis (**Fig. 1A-B**). To ensure that the vanadate-induced enhancement of cell adhesion loss was primarily dependent on modulation of protein pTyr levels, we reasoned that inhibition of protein tyrosine kinases with genistein should antagonize the vanadate effect. Indeed, genistein completely ameliorated cell rounding and apoptosis of RPTE caused by DCVC/vanadate combination (**Fig 1A-B**).

Renal cell injury caused by DCVC is associated with differential protein tyrosine phosphorylation

The data described above indicated that DCVC causes an imbalance in protein tyrosine

kinase and phosphatase activity, which was causally linked to renal cell detachment and the onset of apoptosis. Next, we evaluated DCVC-induced alterations in total protein pTyr status by Western blotting for general tyrosine phosphorylation. DCVC caused a decrease in tyrosine-phosphorylation of several proteins (around 70 and 120 kDa) in a time dependent manner (**Fig. 1C**). Genistein partly prevented the decrease in protein pTyr caused by DCVC. In contrast, inhibition of phosphatase activity with vanadate resulted in a strong increase in tyrosine phosphorylation when cells were treated with DCVC (**Fig. 1C**). This increase was already evident at 4 h when cell detachment was just initiated but no apoptosis was yet detected. Vanadate alone did not affect protein tyrosine phosphorylation. Importantly, the vanadate-induced increase in pTyr in RPTE cells was completely prevented by genistein, suggesting that DCVC primarily modifies tyrosine kinase activity. Similar observations were made when freshly isolated proximal tubular cells were exposed to DCVC in the presence of vanadate (data not shown), indicating that the DCVC-induced imbalance in tyrosine kinase and phosphatase activity is also relevant for proximal tubular cells with a proteome profile that directly reflects the *in vivo* condition.

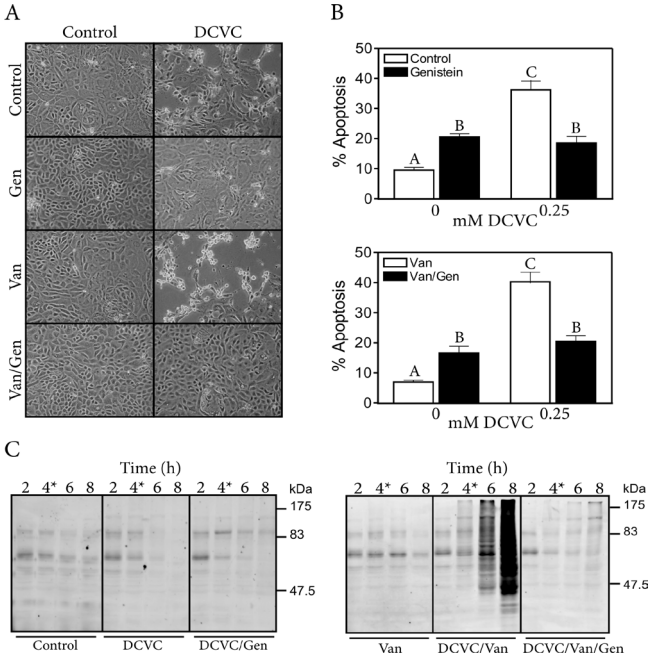

Figure 1. *DCVC-induced cell rounding and apoptosis is regulated by tyrosine kinases.* RPTE were treated with DCVC (0.25 mM) in the presence or absence of vanadate (Van, 25 μM) and/or genistein (Gen, 100 μM). After 4 h incubation, phase-contrast images were taken of control and treated cells (A). After 8 h of incubation, apoptosis was determined using flow cytometry analysis (B). At 4h samples were taken for 1D western blotting and analyzed for tyrosine phosphorylation using anti-tyrosine antibody (PY99). Changes in pTyr after DCVC exposure were studied in time in either the absence or the presence of Gen or Van (C). Data shown represent the mean ± S.E.M. for three independent experiments (n=3) and the letters indicate statistical differences ($p<0.05$).

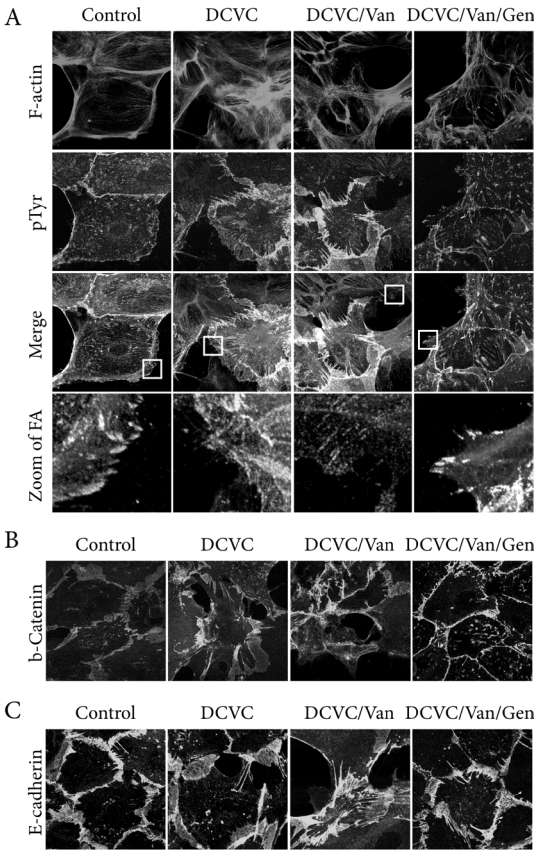

Figure 2. *DCVC exposure results in F-actin reorganization and translocation of tyrosine phosphorylated proteins.* RPTE were exposed to DCVC (0.25 mM) for 4 h in the presence or absence of vanadate (Van, 25 μM) and/or genistein (Gen, 100 μM). Thereafter RPTE were fixed and double-stained for tyrosine phosphorylation (PY99) and F-actin (rhodamin/phalloidin) (A), β-catenin (B) or E-cadherin (C) followed by confocal laser scanning microscopy. Inserts represent enlarged focal adhesions. Images shown are representative of three independent experiments (n=3).

DCVC-induced cell detachment is preceded by changes in localization of pTyr proteins at cell-cell and cell-ECM contacts

Our data indicate that the imbalance in protein tyrosine kinase and phosphatase activity caused by DCVC is responsible for the DCVC-induced morphological changes of RPTE. Since, nephrotoxicant-induced renal cell injury often results in alterations of the F-actin cytoskeletal network organization we analyzed whether DCVC-induced morphological changes corresponded to F-actin rearrangements that are linked to changes in localization of pTyr proteins. RPTE were double stained for pTyr and F-actin (**Fig. 2A**). Four hours exposure to DCVC caused considerable F-actin rearrangement, characterized by loss of thick F-actin bundles and condensation of F-actin into large F-actin clusters. The F-actin changes were related to alterations in protein pTyr at the sites of cell adhesion: while in untreated cells we observed a specific localization of pTyr staining at the focal adhesions (FAs) and adherens junctions (AJs), exposure of RPTE to DCVC resulted in loss of pTyr staining from the FAs (**Fig. 2A**, inserts), possibly due to the reorganization of these structures. Inhibition of tyrosine phosphatases by vanadate resulted in enhanced DCVC-induced disruption of the FAs. This disruption was not completely prevented by genistein, as determined by the redistribution of FAK (data not shown).

In contrast to DCVC-induced loss of pTyr from the FAs, pTyr was increased at AJ and located in broad plaques in cells that still formed cell-cell interactions after DCVC exposure (**Fig. 2A**). Vanadate further enhanced protein pTyr prior to disruption of AJs (**Fig. 2A**), while both the increase in protein pTyr at cell-cell junctions and as well as the disruption of F-actin organization were completely ameliorated by genistein (**Fig. 2A**). Since the formation of stable cell-cell interactions depends on maintaining AJ proteins such as β-catenin and E-cadherin in a dephosphorylated state DCVC may cause translocation of these proteins thereby facilitating the onset of apoptosis. Immunofluorescence revealed indeed a redistribution of both proteins, normally comprising the AJ, away from the plasma membrane to the cytoplasm upon detachment of RPTE cells after DCVC and DCVC/Van (**Fig. 2B-C**). In cells that still formed cell-cell interactions, we observed broader plaques of β-catenin and E-cadherin at these interactions, compared to control RPTE. The redistribution of E-cadherin and β-catenin was prevented when blocking kinase activity with genistein.

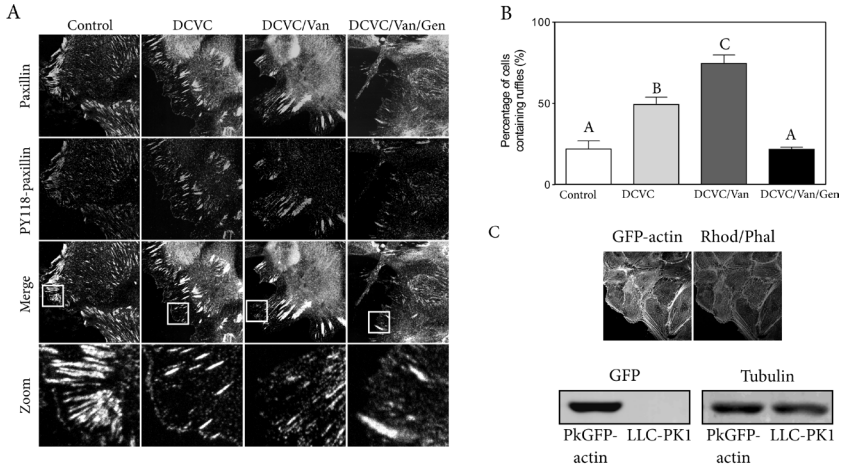

Figure 3A-C. *DCVC-induced lamellipodia formation is inhibited by genistein and enhanced by vanadate.* RPTE were exposed to DCVC (0.25 mM) for 4 h in the presence or absence of genistein (Gen, 100 μM) and/or vanadate (Van, 25 μM). Thereafter RPTE were fixed and stained for paxillin and PY118-paxillin followed by confocal laser scanning microscopy (A). In sub-confluent cultures the percentage of cells that formed lamellipodia as part of the total amount of cells that could form lamellipodia (cells on the edges of small groups) was calculated (B). LLC-PK1 cells were stably transfected with GFP-actin (pkGFP-actin) and evaluated by immunofluorescence and Western blotting (C). Images shown are representative of three independent experiments (n=3) and the letters indicate statistical differences ($p<0.05$).

DCVC-induced lamellipodia formation is tyrosine kinase dependent

In addition to the DCVC-induced changes in F-actin fibers and cell adhesion sites, we observed formation of membrane ruffles or so-called lamellipodia in RPTE cells that were treated with DCVC. To analyze for lamellipodia formation, RPTE cells were stained for paxillin and tyrosine phosphorylated paxillin, a protein that is localized at newly formed

focal complexes at the lamellipodia [32]. DCVC caused formation of lamellipodia (**Fig. 3A-B**, arrows indicate newly formed lamellipodia) at 4 h prior to the onset of apoptosis. This lamellipodia formation was dependent on protein tyrosine kinase activity since inhibition of phosphatases by vanadate promoted lamellipodia formation, while genistein prevented this formation (**Fig. 3A-B**).

The formation of lamellipodia is driven by active F-actin reorganization. To obtain more detailed information of the dynamics the lamellipodia in relation to DCVC-induced cytoskeletal changes, we performed live cell imaging using the well-characterized renal epithelial cell line LLC-PK1. The mechanism of DCVC-induced cytotoxicity in similar in LLC-PK1 cells and RPTE cells [9]. The LLC-PK1 cells allow the expression of GFP-tagged proteins. To study the dynamics of DCVC-induced lamellipodia formation and F-actin reorganization, GFP-actin was stably expressed in LLC-PK1 cells (pkGFP-actin) (**Fig. 3C**). The pkGFP-actin cells were exposed to DCVC and actin dynamics was followed for 4 h (**Fig. 3C**). Control pkGFP-actin cells showed little rearrangement in their F-actin stress fiber network, whereas small lamellipodia were formed as a result of random movement. In contrast, DCVC treatment resulted in a strong reorganization of the F-actin cytoskeletal network within the pkGFP-actin cells (**Fig. 3D**, zoom left) with formation of large F-actin stress fiber clusters as was observed in the RPTE cells (**Fig.2A**). In addition, DCVC caused a rapid formation of lamellipodia with GFP-actin localization in newly formed lamellipodia. F-actin fibers were formed and reorganized as the lamellipodia extended into a broad lamellipod (**Fig. 3D**, zoom right).

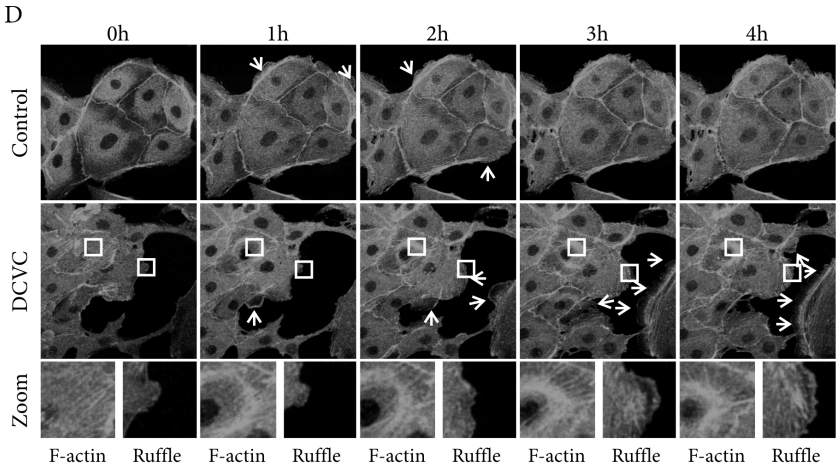

Figure 3D. *DCVC-induced lamellipodia formation and actin reorganization.* The dynamics of F-actin reorganization and lamellipodia formation was imaged for 4 h in pkGFP-actin cells exposed to DCVC. Frames were selected to depict cell shape changes at 0, 1, 2, 3 and 4 h (D). Arrows indicate newly formed lamellipodia, zooms are depicted of DCVC-induced F-actin fiber reorganization (left) and lamellipodia formation (right). Images shown are representative of three independent experiments (n=3) and the letters indicate statistical differences ($p<0.05$).

Protein tyrosine phosphorylation profiling of DCVC-exposed RPTE cells

So far, our results demonstrate that DCVC-induced cell detachment and apoptosis, which is preceded by F-actin rearrangement and lamellipodia formation, is regulated by tyrosine kinase activity. Thus, it would be essential to identify tyrosine phosphorylated proteins that are linked to the effects mediated by DCVC. To screen for differentially phosphorylated proteins after DCVC treatment we used phospho-tyrosine proteomic analysis (two-dimensional SDS-PAGE (2D) in conjunction with 2D immunoblot analysis with anti-pTyr antibody detection) to identify the proteins with a change in tyrosine phosphorylation before the onset of renal cell injury.

For 2D pTyr protein profiling four groups were used: control, DCVC, DCVC/Van and DCVC/Van/Gen. In this way we were able to identify phospho-tyrosine proteins affected by DCVC alone, but also obtain detailed information on changes in tyrosine phosphorylation during DCVC-induced renal cell injury in the absence of either tyrosine phosphatase or tyrosine kinase activity. All RPTE cells were exposed for 4 h; a time point before the onset of cell detachment and apoptosis. Protein samples were separated according to MW and pI, transferred to membranes followed by pTyr detection using PY99 antibody (**Fig. 4A-B**). Matching of spots from triplicate blots in PDQuest software resulted in detection of 50-57 pTyr spots in total, of which 25 spots could be matched to a corresponding protein spot on the preparative Sypro ruby gel (**Fig. 4**). For the remaining spots, the Sypro ruby intensity (i.e. protein amount) was too low. Using MALDI-TOF-MS analysis we identified both proteins with a changed as well as with an unchanged pTyr status. Knowledge of both groups could increase our understanding in the role of protein tyrosine phosphorylation in either normal or injured renal cells. Only three spots could not be identified, possibly due to their low protein concentration even though the tyrosine phosphorylation signals were strong. The identified proteins included: 1) cytoskeleton-related proteins, like actin-related protein 2 (Arp2) and 3 (Arp3), cytokeratin 8, t-complex protein 1, chaperone containing TCP-1 and gelsolin precursor; 2) stress response proteins, such as HSC70; 3) transcription and translation control proteins, including nuclear ribonucleoprotein A2/B1; and 4) proteins involved in metabolism, including pyruvate kinase and glucose-6-phosphate dehydrogenase (G6PDH) (Table 1). The major differentially phosphorylated proteins were Arp2, G6PDH and a yet unidentified protein (spot 3). Treatment of RPTE with DCVC and vanadate did not change the overall 2D pTyr profile, but rather showed differences in signal intensities. In particular, phospho-spots 3, 8, 9, 11, 12 and 13 showed an enhanced tyrosine phosphorylation when blocking tyrosine phosphatases. G6PDH (spot 9) was already phosphorylated in DCVC treated cells, whereas programmed cell death-6-interacting protein (spot 8) could now be recognized as differentially phosphorylated proteins in DCVC-induced renal cell-injury. Instead of an increase in pTyr, the phospho-proteins Arp2, pyruvate kinase, ribonucleoprotein, cytokeratin 8 and HSC 70 showed a decrease in pTyr, possibly due to changes in the dynamics of activation of signal transduction pathways when blocking phosphatase activity. Finally, genistein decreased the pTyr status of a subset of proteins, including pyruvate kinase, G6PDH, Arp2 and programmed cell death 6 interacting protein.

Table 1: *Data analysis of all phospho-protein spots subjected for MALDI-TOF-MS identification*

Spot No.	Control[a]	DCVC[1]	DCVC/Van[2]	DCVC/Van/Gen[3]	Protein name	pI	Mw (kDa)	Protein function
1	11862	2.8	-2.1	2.6	Nuclear ribonucleoprotein A2/B1	8.67	36.0	Transcription and translation control
2	12896	1.4	-1.7	-1.9	Nuclear ribonucleoprotein A2/B1	8.67	36.0	Transcription and translation control
3	700	11.0	14.5	2.9	Not identified			
4	345	17.4	9.8	7.0	Actin-related protein 2	8.39	52.8	Cytoskeleton regulator
5	3112	1.9	-1.3	2.0	S-adenosylhomocysteine hydrolase	6.07	47.5	Metabolism
6	1796	4.2	2.6	1.8	Pyruvate kinase, M2 isoenzyme	7.15	57.8	Metabolism
7	1299	3.2	2.3	1.2	Chaperonin containing TCP-1	6.45	55.7	Chaperone/Cytoskeleton regulator
8	2566	1.5	2.7	-1.2	Programmed cell death 6 interacting protein	7.45	70.5	Cytoskeleton regulator
9	538	9.4	13.4	3.7	Glucose-6-phosphate dehydrogenase	6.19	54.9	Metabolism
10	26039	-1.6	-1.5	-2.7	Collapsin response mediator protein 4 (CRMP4)	6.04	61.9	Chaperone/Cytoskeleton regulator
11	12056	-1.1	2.2	1.2	t-complex protein-1	5.86	60.3	Chaperone/Cytoskeleton regulator
12	2268	-3.7	4.7	1.8	t-complex protein-1	5.86	60.3	Chaperone/Cytoskeleton regulator
13	2737	1.1	2.5	-1.2	Not identified			
14	2381	-1.1	1.4	1.6	Actin-related protein 3 homolog	8.85	55.3	Cytoskeleton regulator
15	23004	1.0	-2.1	2.1	Cytokeratin 8	5.49	52.7	Cytoskeleton regulator
16	8606	1.0	-1.4	1.8	Keratin complex 2	5.67	50.8	Cytoskeleton regulator
17	13122	1.1	-2.0	1.4	Keratin complex 2	5.67	50.8	Cytoskeleton regulator

Spot No.	Control[a]	DCVC[1]	DCVC/Van[2]	DCVC/Van/Gen[3]	Protein name	pI	Mw (kDa)	Protein function
18	2562	3.7	1.4	3.2	Cytokeratin 8	5.49	52.7	Cytoskeleton regulator
19	2901	2.1	2.3	1.6	Gelsolin precursor (actin depolymerizing factor)	6.22	84.9	Cytoskeleton regulator
20	16687	-1.5	-1.2	Not present	Not identified			
21	14170	-1.2	1.6	Not present	Heterogeneous nuclear ribonucleo-protein K	5.39	51.0	Transcription and translation control
22	12443	-1.1	1.5	Not present	Heterogeneous nuclear ribonucleo-protein K	5.39	51.0	Transcription and translation control
23	14461	1.6	1.3	Not present	Unnamed protein product (Hsp60 family member)			Stress response
24	29140	-2.0	-1.2	-2.2	Heat shock cognate protein 70	5.44	69.5	Stress response
25	51490	-3.1	-2.8	-2.7	Heat shock cognate protein 70	5.44	69.5	Stress response

[a] Average spot intensity of control blots (n=3)

[1] Average fold differences, obtained by dividing averaged spot intensities of DCVC exposed cells by averaged spot intensities of control cells

[2] Average fold differences, obtained by dividing averaged spot intensities of DCVC/Vanadate exposed cells by averaged spot intensities of control cells

[3]Average fold differences, obtained by dividing averaged spot intensities of DCVC /Vanadate/Genistein exposed cells by averaged spot intensities of control cells

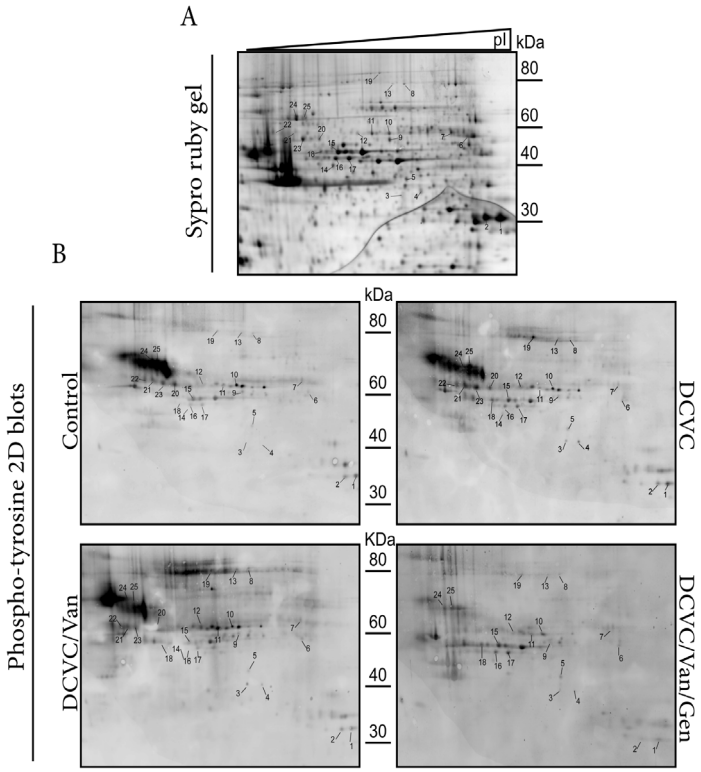

Figure 4. *2-Dimensional protein tyrosine profiling of DCVC-exposed RPTE.* RPTE were treated with DCVC (0.25 mM) in the presence or absence of vanadate (Van, 25 μM) or vanadate/genistein (Van/Gen, 25/100 μM) for 4 h and thereafter harvested for 2D-electrophoresis. For both treated and control cell lysates four 2D gels were run; one preparative Sypro ruby stained gel (A) and 3 gels for transfer of proteins to nitrocellulose membranes (B). The 2D Western blots were probed with anti-tyrosine antibody (PY99). Phospho-tyrosine patterns were visualized using ECL plus followed by scanning with a Typhoon 9400. All blots were run in triplicate and analyzed using PDQuest software followed by spot picking and MALDI-TOF-MS identification (See also **Table 1**).

Tyrosine phosphorylation of Arp2 precedes DCVC-induced apoptosis

Arp2 was identified as the major differentially tyrosine phosphorylated protein during DCVC-induced RPTE cell injury. Since Arp2 regulates the assembly and maintenance of many actin-based structures in the cell as part of the Arp2/3 complex, we further evaluated this protein. The phosphor-tyrosine content of Arp2 increased 17 times after DCVC treatment and was inhibited by genistein/vanadate treatment (**Fig. 5A**). To confirm the tyrosine phosphorylation of Arp2 in RPTE cells, 2D blots were reprobed for Arp2 (**Fig. 5B**). Two Arp2 spots were visualized of which the right spot co-localized with tyrosine spot number 4, which was identified as Arp2 by MS analysis. Interestingly, spot number 3, which could not be identified by MS analysis, also co-localized with Arp2. The pTyr of this spot increased after DCVC-vanadate combination treatment, whereas the pTyr

content of spot 4 decreased under these conditions. This suggests that Arp2 is phosphorylated on an additional Tyr site after DCVC-Van treatment, thereby generating a more negative protein charge causing the spot to shift to the acidic site of the gel (**Fig. 5B**). In addition, DCVC increased the tyrosine phosphorylation status of Arp2 in the pkGFP-actin cells (**Fig. 5C**), which were used for live-cell imaging (**Fig. 3C**). Although we also identified Arp3 as a phosphotyrosine protein, no significant changes were observed in its tyrosine phosphorylation status.

The Arp2/3 complex components localize at lamellipodia [33] and are required for actin filament branching and lamellipodia extension. As described above, DCVC caused lamellipodia formation in both RPTE as well as pkGFP-actin cells. Arp2 is localized in the lamellipodia that were formed early after DCVC exposure (**Fig. 5D**) at the time point at which the phospho-tyrosine content of Arp2 was increased (**Fig. 5C**). Expression of GFP-Arp2 was cytotoxic for the LLC-PK1 cells, making it impossible to study the wild-type protein or one of its phospho-specific mutants in live cells in the context of mechanisms of DCVC-induced cytotoxicity. Together our data show that the nephrotoxicant DCVC caused tyrosine kinase-dependent lamellipodia formation, which is linked to increased tyrosine phosphorylation of the actin regulatory protein Arp2. These events precede actin-regulated cell detachment and apoptosis, which in turn are also dependent on increased tyrosine kinase activity.

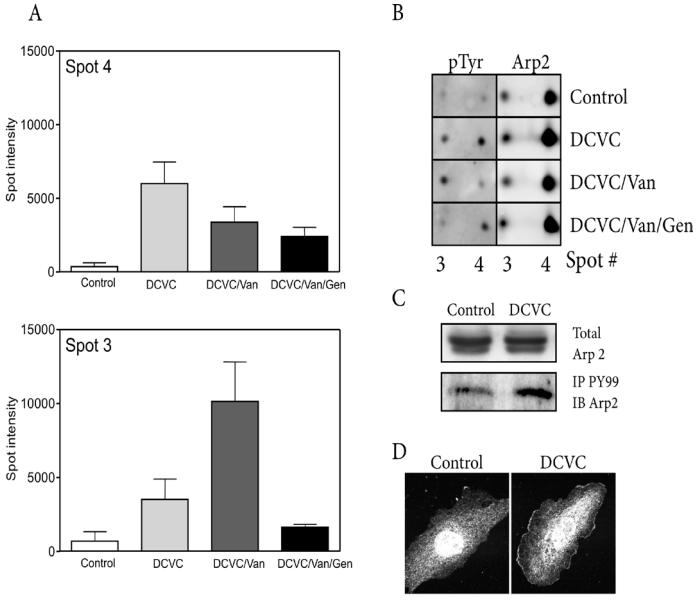

Figure 5. *Verification of DCVC-induced Arp2 tyrosine phosphorylation.* Tyrosine spot intensities of Arp2 (spot #3 and 4) were calculated using PDQuest analysis (A). 2D anti-tyrosine Western blots of RPTE cells were reprobed for Arp2 (B). LLC-PK1 cells were exposed to DCVC (1mM) for 4 h. After IP of pTyr proteins using PY99-agarose beads and SDS-PAGE, blots were probed with anti-Arp2 antibody (C). To determine the localization of Arp2 in LLC-PK1 cells were exposed to DCVC for 4 h, fixated and stained for Arp2 followed by confocal laser scanning microscopy (D).

DISCUSSION

In the present study, we examined the role of altered protein tyrosine phosphorylation in toxicant-induced renal cell injury and identified proteins with a change in tyrosine phosphorylation status prior to renal cell injury. We were able to 1) show that DCVC-induced cell detachment and apoptosis was blocked by genistein, a general tyrosine kinase inhibitor and enhanced by vanadate, a general tyrosine phosphatase inhibitor; 2) demonstrate that the onset of DCVC-induced apoptosis was preceded by increased tyrosine phosphorylation of a subset of proteins when inhibiting phosphatase activity, which was blocked by genistein; and 3) identify proteins with a change in tyrosine phosphorylation status during renal cell injury using phospho-tyrosine proteomics. These differentially phosphorylated proteins included 1) cytoskeleton-related proteins, like actin-related protein 2 (Arp2), cytokeratin 8, t-complex protein 1, chaperone containing TCP-1 and gelsolin precursor; 2) stress response proteins, such as HSC70; 3) transcription and translation control proteins, including nuclear ribonucleoprotein A2/B1; and 4) proteins involved in metabolism, including pyruvate kinase and glucose-6-phosphate dehydrogenase (G6PDH). The identification of Arp2, a component of the Arp2/3 complex, as a major alternatively tyrosine phosphorylated proteins seems directly associated with the DCVC-induced formation of lamellipodia early after treatment.

The tyrosine phosphorylation content of Arp2, the major differentially phosphorylated protein in this study, was approximately 17 times higher after DCVC exposure (**Fig. 5A**). Arp2 is a member of the Arp2/3 complex. While Arp2 was phosphorylated in DCVC exposed RPTE, the phosphorylation of Arp3 was not affected. The Arp2/3 complex is important for the assembly and maintenance of actin-based structures in the cell and localizes in lamellipodia during cell shape changes. The Arp2/3 complex is activated by cortactin or N-WASP through protein tyrosine kinase pathways [33,34]. In addition, the Arp2/3 complex is able to recruit actin-related proteins, such as vinculin and E-cadherin [35]. Apoptosis is generally preceded by profound changes of the actin cytoskeleton. DCVC-induced cell detachment and apoptosis was preceded by dynamic rearrangements in the F-actin cytoskeleton and formation of lamellipodia. Inhibition of phosphatase activity by vanadate resulted in enhanced lamellipodia formation during DCVC exposure, which was completely inhibited by genistein, a general tyrosine kinase inhibitor (**Fig. 5C**). Since Arp2/3 complex is able to localize in lamellipodia and its tyrosine phosphorylation was affected by DCVC, we propose an essential function for (tyrosine phosphorylated) Arp2 in toxicant-induced cytoskeletal rearrangement preceding renal cell apoptosis. This fits with a genistein-mediated inhibition of DCVC-induced Arp2 phosphorylation, lamellipodia formation and apoptosis.

We observed a DCVC-induced increase in tyrosine phosphorylation of Arp2 upon rearrangement of the F-actin cytoskeletal network, which was decreased by inhibition of tyrosine kinase activity. DCVC and vanadate combination treatment caused a shift of phosphorylated Arp2 to the acidic side of the gel suggesting that Arp2 is phosphorylated on an additional Tyr site after DCVC-Van treatment Arp2 as well as Arp3 have been identified as differentially tyrosine phosphorylated proteins in relation to growth

factor-induced F-actin rearrangement [36,37]. Both EGF as well as PDGF stimulated tyrosine phosphorylation of Arp2/3 to a similar extent in human mesenchymal stem cells. Whether DCVC-induced Arp2 phosphorylation is also dependent on EGFR activation is yet unclear. However, both 2,3,5-Tris-(glutathion-S-yl)hydroquinone (TGHQ) [38] as well as DCVC cause activation of ERK1/2 in LLC-PK1 cells (our own observation and [39]).

Although tyrosine phosphorylation of Arp2/3 was recognized in several cell systems, the tyrosine phosphorylation sites in Arp2/3 remain unknown. Using NetPhos 2.0, a sequence-based prediction database for protein phosphorylation sites, we could identify five tyrosine residues (*e.g.* Y28, 130, 136, 201, 221) as potential tyrosine phosphorylation sites in Arp2. The cytotoxicity of GFP-Arp2 for our LLC-PK1 cells makes it at this moment difficult to study the role of phospho-specific mutants of Arp2 in relation to renal cell injury.

In addition to Arp2, we have also identified several other proteins that were differentially phosphorylated and important in the control of the actin cytoskeletal network, including chaperone containing TCP1, t-complex protein and gelsolin. In a previous study [40], we identified several F-actin regulatory proteins as differentially expressed proteins prior to DCVC-induced apoptosis, including cofilin, Hsp27 and alphaB-crystallin. The turn-over of F-actin, which is also needed for formation of lamellipodia, is regulated by a close collaboration between cofilin, gelsolin and the Arp2/3 complex [41,42]. Together this suggests that the observed F-actin reorganization prior to DCVC-induced cell detachment and apoptosis is regulated by a coordinated (in)activation of these actin cytoskeletal proteins.

In summary, our data show that tyrosine-phosphorylation plays an important role in DCVC-induced renal cell detachment and apoptosis. Phospho-tyrosine proteomic analysis is a valuable tool to identify proteins involved in different cellular processes (*e.g.* apoptosis, cell migration, and tumor metastasis), thereby providing information on signal transduction pathways involved in these processes. In addition, phospho-proteomics may be used in drug toxicity to shed light on the protein networks that are affected during toxicant exposure, thereby enabling prediction of toxicity [43]. Some of the proteins identified in this study might be crucial in the mechanism of both loss of cell adhesion and apoptosis during nephrotoxicity. Assessing the role of proteins such as Arp2 enables a better understanding of the mechanisms of renal cell injury in renal diseases and may also shed light on reactive metabolite-induced toxicities in other target organs.

ACKNOWLEDGEMENTS

We thank the members of the Division of Toxicology of the Leiden/Amsterdam Center for Drug Research for valuable discussion and support.

REFERENCE LIST

1. Lieberthal, W., Koh, J. S., and Levine, J. S. Necrosis and apoptosis in acute renal failure. Semin.Nephrol., 18 : 505-518, 1998.

2. Savill, J. Apoptosis and the kidney. J.Am.Soc. Nephrol., 5: 12-21, 1994.

3. Ueda, N. and Shah, S. V. Tubular cell damage in acute renal failure-apoptosis, necrosis, or both. Nephrol.Dial.Transplant., 15: 318-323, 2000.

4. Frisch, S. M. and Francis, H. Disruption of epithelial cell-matrix interactions induces apoptosis. J.Cell Biol., 124: 619-626, 1994.

5. Bates, R. C., Buret, A., van Helden, D. F., Horton, M. A., and Burns, G. F. Apoptosis induced by inhibition of intercellular contact. J.Cell Biol., 125: 403-415, 1994.

6. van de Water B., Jaspers, J. J., Maasdam, D. H., Mulder, G. J., and Nagelkerke, J. F. *In vivo* and *in vitro* detachment of proximal tubular cells and F-actin damage: consequences for renal function. Am.J.Physiol, 267: F888-F899, 1994.

7. van de Water B., Kruidering, M., and Nagelkerke, J. F. F-actin disorganization in apoptotic cell death of cultured rat renal proximal tubular cells. Am.J.Physiol, 270: F593-F603, 1996.

8. van de Water B., Houtepen, F., Huigsloot, M., and Tijdens, I. B. Suppression of chemically induced apoptosis but not necrosis of renal proximal tubular epithelial (LLC-PK1) cells by focal adhesion kinase (FAK). Role of FAK in maintaining focal adhesion organization after acute renal cell injury. J.Biol.Chem., 276: 36183-36193, 2001.

9. van de Water B., Nagelkerke, J. F., and Stevens, J. L. Dephosphorylation of focal adhesion kinase (FAK) and loss of focal contacts precede caspase-mediated cleavage of FAK during apoptosis in renal epithelial cells. J.Biol.Chem., 274: 13328-13337, 1999.

10. Goligorsky, M. S., Lieberthal, W., Racusen, L., and Simon, E. E. Integrin receptors in renal tubular epithelium: new insights into pathophysiology of acute renal failure. Am.J.Physiol, 264: F1-F8, 1993.

11. Bergin, E., Levine, J. S., Koh, J. S., and Lieberthal, W. Mouse proximal tubular cell-cell adhesion inhibits apoptosis by a cadherin-dependent mechanism. Am.J.Physiol Renal Physiol, 278: F758-F768, 2000.

12. Thadhani, R., Pascual, M., and Bonventre, J. V. Acute renal failure. N.Engl.J.Med., 334: 1448-1460, 1996.

13. Volberg, T., Zick, Y., Dror, R., Sabanay, I., Gilon, C., Levitzki, A., and Geiger, B. The effect of tyrosine-specific protein phosphorylation on the assembly of adherens-type junctions. EMBO J., 11: 1733-1742, 1992.

14. Roura, S., Miravet, S., Piedra, J., Garcia, d. H., and Dunach, M. Regulation of E-cadherin/Catenin association by tyrosine phosphorylation. J.Biol.Chem., 274: 36734-36740, 1999.

15. Hildebrand, J. D., Schaller, M. D., and Parsons, J. T. Identification of sequences required for the efficient localization of the focal adhesion kinase, pp125FAK, to cellular focal adhesions. J.Cell Biol., 123: 993-1005, 1993.

16. Wang, Y. H., Li, F., Schwartz, J. H., Flint, P. J., and Borkan, S. C. c-Src and HSP72 interact in ATP-depleted renal epithelial cells. Am.J.Physiol Cell Physiol, 281: C1667-C1675, 2001.

17. Schwartz, J. H., Shih, T., Menza, S. A., and

Lieberthal, W. ATP depletion increases tyrosine phosphorylation of β-catenin and plakoglobin in renal tubular cells. J.Am.Soc.Nephrol., 10: 2297-2305, 1999.

18. Novogrodsky, A., Weisspapir, M., Patya, M., Meshorer, A., and Vanichkin, A. Tyrphostin 4-nitrobenzylidene malononitrile reduces chemotherapy toxicity without impairing efficacy. Cancer Res., 58: 2397-2403, 1998.

19. Hagar, H., Ueda, N., and Shah, S. V. Tyrosine phosphorylation in DNA damage and cell death in hypoxic injury to LLC-PK1 cells. Kidney Int., 51: 1747-1753, 1997.

20. Richardson, A. and Parsons, T. A mechanism for regulation of the adhesion-associated proteintyrosine kinase pp125FAK. Nature, 380: 538-540, 1996.

21. Braga, V. M. Cell-cell adhesion and signalling. Curr.Opin.Cell Biol., 14: 546-556, 2002.

22. Zheng, X. M., Resnick, R. J., and Shalloway, D. Mitotic Activation of Protein-tyrosine Phosphatase α and Regulation of Its Src-mediated Transforming Activity by Its Sites of Protein Kinase C Phosphorylation. J.Biol.Chem., 277: 21922-21929, 2002.

23. Soskic, V., Gorlach, M., Poznanovic, S., Boehmer, F. D., and Godovac-Zimmermann, J. Functional proteomics analysis of signal transduction pathways of the platelet-derived growth factor β receptor. Biochemistry, 38: 1757-1764, 1999.

24. Chen, J. C., Stevens, J. L., Trifillis, A. L., and Jones, T. W. Renal cysteine conjugate β-lyase-mediated toxicity studied with primary cultures of human proximal tubular cells. Toxicol.Appl. Pharmacol., 103: 463-473, 1990.

25. Groves, C. E., Hayden, P. J., Lock, E. A., and Schnellmann, R. G. Differential cellular effects in the toxicity of haloalkene and haloalkane cysteine conjugates to rabbit renal proximal tubules. J.Biochem.Toxicol., 8: 49-56, 1993.

26. Cummings, B. S., Zangar, R. C., Novak, R. F., and Lash, L. H. Cytotoxicity of trichloroethylene and S-(1, 2-dichlorovinyl)-L-cysteine in primary cultures of rat renal proximal tubular and distal tubular cells. Toxicology, 150: 83-98, 2000.

27. van de Water B., Zoeteweij, J. P., de Bont, H. J., Mulder, G. J., and Nagelkerke, J. F. Role of mitochondrial Ca2+ in the oxidative stress-induced dissipation of the mitochondrial membrane potential. Studies in isolated proximal tubular cells using the nephrotoxin 1,2-dichlorovinyl-L-cysteine. J.Biol.Chem., 269: 14546-14552, 1994.

28. Stevens, J. L., Robbins, J. D., and Byrd, R. A. A purified cysteine conjugate β-lyase from rat kidney cytosol. Requirement for an α-keto acid or an amino acid oxidase for activity and identity with soluble glutamine transaminase K. J.Biol.Chem., 261: 15529-15537, 1986.

29. Hayden, P. J. and Stevens, J. L. Cysteine conjugate toxicity, metabolism, and binding to macromolecules in isolated rat kidney mitochondria. Mol.Pharmacol., 37: 468-476, 1990.

30. Boogaard, P. J., Mulder, G. J., and Nagelkerke, J. F. Isolated proximal tubular cells from rat kidney as an *in vitro* model for studies on nephrotoxicity. I. An improved method for preparation of proximal tubular cells and their functional characterization by α-methylglucose uptake. Toxicol.Appl.Pharmacol., 101: 135-143, 1989.

31. Gorg, A., Postel, W., and Gunther, S. The current state of two-dimensional electrophoresis with immobilized pH gradients. Electrophoresis, 9: 531-546, 1988.

32. Blagoev, B., Ong, S. E., Kratchmarova, I., and Mann, M. Temporal analysis of phosphotyrosine-dependent signalling networks by quantitative proteomics. Nat.Biotechnol., 22: 1139-1145, 2004.

33. Machesky, L. M. and Gould, K. L. The Arp2/3 complex: a multifunctional actin organizer. Curr.Opin.Cell Biol., 11: 117-121, 1999.

34. Millard, T. H., Sharp, S. J., and Machesky, L. M. Signalling to actin assembly via the WASP (Wiskott-Aldrich syndrome protein)-family proteins and the Arp2/3 complex. Biochem.J., 380: 1-17, 2004.

35. Kovacs, E. M., Goodwin, M., Ali, R. G., Paterson, A. D., and Yap, A. S. Cadherin-directed actin assembly: E-cadherin physically associates with the Arp2/3 complex to direct actin assembly in nascent adhesive contacts. Curr.Biol., 12: 379-382, 2002.

36. Blagoev, B., Ong, S. E., Kratchmarova, I., and Mann, M. Temporal analysis of phosphotyrosine-dependent signalling networks by quantitative proteomics. Nat.Biotechnol., 22: 1139-1145, 2004.

37. Kratchmarova, I., Blagoev, B., Haack-Sorensen, M., Kassem, M., and Mann, M. Mechanism of divergent growth factor effects in mesenchymal stem cell differentiation. Science, 308: 1472-1477, 2005.

38. Dong, J., Ramachandiran, S., Tikoo, K., Jia, Z., Lau, S. S., and Monks, T. J. EGFR-independent activation of p38 MAPK and EGFR-dependent activation of ERK1/2 are required for ROS-induced renal cell death. Am.J.Physiol Renal Physiol, 287: F1049-F1058, 2004.

39. Vaidya, V. S., Shankar, K., Lock, E. A., Dixon, D., and Mehendale, H. M. Molecular mechanisms of renal tissue repair in survival from acute renal tubule necrosis: role of ERK1/2 pathway. Toxicol.Pathol., 31: 604-618, 2003.

40. de Graauw, M., Tijdens, I., Cramer, R., Corless, S., Timms, J. F., and van de, W. B. Heat shock protein 27 is the major differentially phosphorylated protein involved in renal epithelial cellular stress response and controls focal adhesion organization and apoptosis. J.Biol. Chem., %19;280: 29885-29898, 2005.

41. Ressad, F., Didry, D., Egile, C., Pantaloni, D., and Carlier, M. F. Control of actin filament length and turnover by actin depolymerizing factor (ADF/cofilin) in the presence of capping proteins and ARP2/3 complex. J.Biol.Chem., 274: 20970-20976, 1999.

42. DesMarais, V., Macaluso, F., Condeelis, J., and Bailly, M. Synergistic interaction between the Arp2/3 complex and cofilin drives stimulated lamellipod extension. J.Cell Sci., 117: 3499-3510, 2004.

43. Liebler, D. C. and Guengerich, F. P. Elucidating mechanisms of drug-induced toxicity. Nat.Rev.Drug Discov., 4: 410-420, 2005.